FULL LENGTH **ASCHT2021-216**

Numerical prediction for effective thermal conductivity of C/SiC composites by using a multiscale numerical method

Jingyu Guo[a], Zixiang Tong[b,*], Ming-Jia Li[a], Yisi Yu[a]

[a]School of Energy and Power Engineering, Xi'an Jiaotong University, Xi'an, 710049, P. R. China
[b]School of Human Settlements and Civil Engineering, Xi'an Jiaotong University, Xi'an, 710049, P. R. China

* Corresponding author, E-mail: zxtong@xjtu.edu.cn

Abstract

To investigate the coupled conduction-radiation heat transfer in C/SiC composites, a multiscale numerical method is proposed in this paper. The multiscale method combines a three-scale physical model and a multiscale mathematical method, which is used to predict the thermal conductivity of composites. Then, an experimental study was conducted to verify the multiscale numerical method proposed herein. Comparing with the experimental data, the average error of the multiscale model is 4.13% for the effective thermal conductivity. The computational time of the multiscale model can be reduced from more than 8 hours to 1.6 hours compared with the traditional model. Therefore, the proposed multiscale model can significantly reduce the computational time of reconstructing temperature and radiation intensity fields while ensuring the computational accuracy. Finally, influences of the key parameters, including porosity, temperature, and carbon fiber volume fraction, on the effective thermal conductivity of C/SiC composites are evaluated. The present work can provide a scientific guidance for the precise design of thermal protection composites.

Keywords: C/SiC composites, Conduction-radiation heat transfer, Effective thermal conductivity, Multiscale numerical method

1. Introduction

C/SiC composites are continuous fiber-reinforced ceramic matrix with many excellent mechanical and physical properties, such as high thermal stability, high strength and toughness, light weight, and excellent thermal shock resistance[1-4]. C/SiC composites are usually used as thermal protection structures of spacecrafts. They would experience complex mechanical and thermal conditions for a long time in huge temperature changing environment[5]. C/SiC composites will suffer fatigue and failure due to the uneven heat flux distribution. Therefore, it is necessary to study their heat transfer performance. C/SiC composites can be divided into three distinct types according to different microstructures, including plain woven composites, 3D stitched composites, and 3D needled composites[6], among which the plain woven composites is the most widely used with low weight and high strength. Thermal conductivity is an important parameter to evaluate the heat transfer performance of thermal protective composites. Considering the complex microstructure of plain woven composites, it is challenging and significant to study their thermal conductivity[7].

Sheikh et al.[8] used laser pulse heating to measure the thermal conductivity of the fiber-reinforced ceramic matrix composites under different heating conditions. Berbon et al.[9] evaluated the effects of heat treatment parameters on the transverse thermal conductivity. However, there are not many experimental studies focusing on the thermal conductivities of plain woven C/SiC composites in literatures because the structure is very complicated and causes high manufacturing cost.

Over past decades, theoretical and numerical methods have been widely devoted to researching the properties of the composites because of their low cost. The thermal conductivity of C/SiC composites can be predicted based on the representative volume element (RVE) model at microscale and mesoscale[10]. A series of theoretical methods can be used to calculate the effective thermal conductivity of the matrix[11-14]. For two-phase composites, the Parallel and Series models define the upper and lower bounds of the effective thermal conductivity[15]. Some theoretical models are developed to study the thermal conductivities of the fiber-reinforced composites[16-19].

Even though theoretical methods effectively predict the thermal conductivities of composites, they apply only to a specific structure or material. In order to overcome the shortcoming, some researchers carried out numerical investigations to predict the effective thermal conductivities of plain woven composites. The finite element homogenization method[20,21] is widely used to predict the effective thermal conductivity of

composites and simulate the distribution of heat flow and temperature inside the composites. Gou et al.[22] studied the temperature distribution in a RVE of three-dimensional and four-directional braided composites with appropriate boundary conditions by the finite element method (FEM) to predict the effective thermal conductivity of the composite. Liu et al.[23] proposed a finite volume numerical model at three scale levels on the basis of 3D geometric reconstructions with in-yarn and out-of-yarn porosities. The thermal conductivities of SiC matrix, woven yarn, and plain woven C/SiC composites are predicted using up-scaling approach. To explore the heat transfer mechanism of composites at macroscale and mesoscale, some researchers simulated the temperature field using a mathematical homogenization method. The cross-scale heat transfer process at macroscale and mesoscale was analyzed by using the multiscale mathematical method. Then, the effective heat transfer properties of composites with periodic structure was obtained [24,25]. The mathematics-based multiscale method is suitable for composites with different structures, which has been widely used in the study of heat and mass transfer of composites with periodic structures[26]. Liu et al.[27] proposed a homogenization-based multiscale method for predicting the effective thermal conductivity of porous materials with radiation, which considers the effect of geometry and distribution of pores. Allaire et al.[28] studied the homogenization of a heat conduction problem in a periodically perforated domain with a nonlinear and nonlocal boundary condition modeling radiative heat transfer in the perforations. Some researchers subsequently developed the model and make it more widely applicable[29-32].

From the above literature review, it can be found that the existing theoretical and experimental models are only applied to specific braided structures or specific fiber and matrix materials. On the other hand, the complex structures of composites have a three-scale feature, which have not yet been considered comprehensively in previous works. Thus, it is necessary to develop a multiscale method that can not only accurately predict the thermal conductivity of different composites, but also study the heat transfer mechanism at three different scales.

The main purpose of this paper is to establish a general multiscale model, which can predict effective thermal conductivity of composites under varying conditions. In section 2, a three-scale physical model of plain woven C/SiC composites is established based on the structural parameters measured. A multiscale coupled conduction-radiation heat transfer mathematical model for predicting effective thermal conductivity of composites is also described. In section 3, empirical formulas and model validation is presented. The effects of carbon fiber volume fraction, porosity and temperature on effective thermal conductivities of plain woven composites are discussed. Finally, conclusions are summarized and proposed in Section 4.

2. Methodology

2.1 Physical model of C/SiC composites

To get the meso-structural geometric parameters of C/SiC composites, the scanning images of the composites are obtained by scanning electron microscope (SEM), as shown in Fig.1. It can be seen that the material is mainly composed of the matrix with pores and fiber yarns. The fiber yarns are arranged in alternative layers, and the adjacent layers are intersected at an angle of 90°, as marked in bule lines and red lines. The cross-section of the yarn is approximately an ellipse. Geometric parameters of the C/SiC composites are listed in Table 1, which are used to reconstruct the physical model of C/SiC composites.

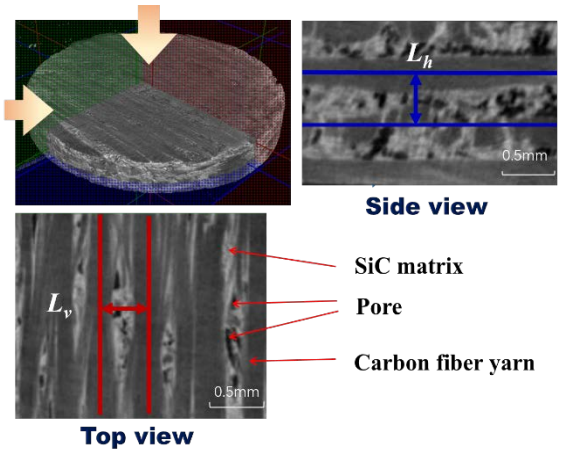

Fig.1 SEM images of C/SiC composites

Table 1 Geometric parameters of C/SiC composites

Major axis of the fiber yarn	Minor axis of the fiber yarn	Horizontal gap between adjacent fiber yarns (L_h)	Vertical gap between adjacent fiber yarns (L_v)
0.45 mm	0.2 mm	0.5 mm	0.48 mm

Considering the complex structure of C/SiC composites, a multiscale method is used to reconstruct the 3D physical structure. The relevant length scales include: (i) whole composite level (macroscale), (ii) RVE level (mesoscale), (iii) pore and fiber level (microscale). Fig.2 demonstrates the three-dimension model of C/SiC composites at each length scale in the multiscale.

The physical properties of C/SiC composites are uniform at macroscale. The physical model at this scale depends on the geometric shape of the whole composites, which cannot reflect the micro structure. The structure of C/SiC composites is periodic at mesoscale, where the RVE is employed to compute the homogenized properties of the composites. The RVE consists of the SiC matrix and yarns (short for carbon fiber yarns). The SiC matrix can be regarded as isotropic due to the random distribution of pores[15], while yarns have obvious anisotropy in both transverse and longitudinal directions. At microscale, the matrix contains small pores and a few large pores. These pores with air are formed during the manufacturing process of the composites[33,34]. The meso-scale yarn is mainly composed of micro-scale carbon fibers and matrix. Notably, air mainly exists in the out-of-yarn SiC matrix, so that less air exists in the in-yarn SiC matrix[23]. Effective thermal conductivities of the matrix and yarns are calculated based on their RVEs. The effective thermal conductivities of the SiC matrix with porosity of 35.5% are predicted in this paper, spherical pores are distributed randomly and uniformly in the matrix. Considering the tight arrangement of the fibers, the fiber volume fraction in the RVE of the fiber yarns is assumed to be 90.69%[35].

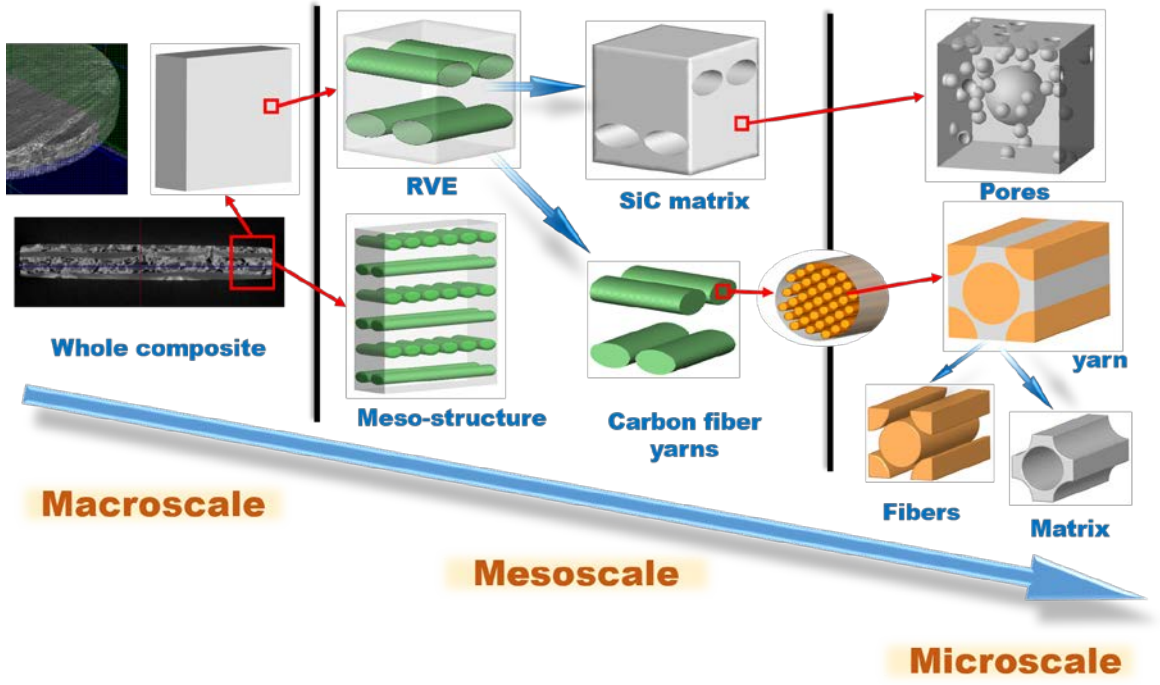

Fig.2 The three-scale physical model of C/SiC composites

2.2 Multiscale conduction-radiation heat transfer mathematical model

2.2.1 Governing equations

The multiscale conduction-radiation heat transfer model proposed by Tong et al.[36] is used to simulate the complex heat transfer process inside the composites. Under high temperature and heat flux, the governing equations of coupled conduction-radiation heat transfer problem are shown in Eq.(1) and Eq.(2):

$$\nabla_{\mathbf{x}} \cdot (\mathbf{\Lambda} \nabla_{\mathbf{x}} T(\mathbf{x})) - \kappa \left(4\sigma_{\mathrm{B}} T(\mathbf{x})^4 - \int_{4\pi} I(\mathbf{x}, \Omega) \mathrm{d}\Omega \right) = 0 \tag{1}$$

$$\boldsymbol{n} \cdot \nabla_{\mathbf{x}} I(\mathbf{x}, \Omega) = -\beta I(\mathbf{x}, \Omega) + \frac{\kappa \sigma_{\mathrm{B}}}{\pi} T(\mathbf{x})^4 + \frac{\sigma_{\mathrm{s}} \Phi}{4\pi} \int_{4\pi} I(\mathbf{x}, \Omega') \mathrm{d}\Omega' \tag{2}$$

where $\mathbf{x}$ is the macroscopic coordinate; Ω is the solid angle; $T(\mathbf{x})$ represents the temperature at the coordinate $\mathbf{x}$; $I(\mathbf{x}, \Omega)$ is the radiative intensity at the coordinate $\mathbf{x}$ along the direction Ω; $\boldsymbol{n}$ is the unit vector along the

direction Ω; $\mathbf{\Lambda}$ is the thermal conductivity matrix; κ is the absorption coefficient; σ_s is the scattering coefficient; β is the extinction coefficient with the relationship $\beta=\kappa+\sigma_s$; Φ is the scattering phase function. In this paper, isotropic scattering is assumed, and the boundary is black with an emissivity of 1.

A multiscale coupled conduction-radiation heat transfer numerical model, which is called as multiscale model for short in the following study, is established by using the homogenization method. ε is defined as the scale of the RVE, and the mesoscale coordinate $\mathbf{y}=\mathbf{x}/\varepsilon$. The temperature and radiative intensity fields are expanded into the following series, as presented in Eq.(3) and Eq.(4):

$$T(\mathbf{x}) = T_0(\mathbf{x},\mathbf{y}) + \varepsilon T_1(\mathbf{x},\mathbf{y}) + \cdots \tag{3}$$

$$I(\mathbf{x},\mathbf{\Omega}) = I_0(\mathbf{x},\mathbf{y},\mathbf{\Omega}) + \varepsilon I_1(\mathbf{x},\mathbf{y},\mathbf{\Omega}) + \cdots \tag{4}$$

The gradient operator can be expressed as:

$$\nabla = \nabla_{\mathbf{x}} + \frac{1}{\varepsilon}\nabla_{\mathbf{y}} \tag{5}$$

The temperature and radiative intensity fields are decomposed into homogenized fields T_0, I_0 and slight fluctuations T_1, I_1. By substituting Eq.(5) into Eq.(3) and Eq.(4), combining and sorting out the coefficients of each order of ε, the governing equations can be obtained.

The equation in the ε^0 order:

$$\nabla_{\mathbf{y}} \cdot \left[\mathbf{\Lambda}(\mathbf{y})\nabla_{\mathbf{y}} T_0(\mathbf{x},\mathbf{y})\right] = 0 \tag{6}$$

It can be concluded from Eq.(6) that T_0 is a function of macroscopic coordinate $\mathbf{x}$:

$$T_0 = T_0(\boldsymbol{x}) \tag{7}$$

The conduction and radiation equations in the ε^{-1} order:

$$\nabla_{\mathbf{x}} \cdot \left(\mathbf{\Lambda}\nabla_{\mathbf{y}} T_0\right) + \nabla_{\mathbf{y}} \cdot \left(\mathbf{\Lambda}\nabla_{\mathbf{x}} T_0 + \mathbf{\Lambda}\nabla_{\mathbf{y}} T_1\right) = 0 \tag{8}$$

$$\boldsymbol{n} \cdot \nabla_{\mathbf{y}} I_0(\mathbf{x},\mathbf{y},\Omega) = 0 \tag{9}$$

Eq.(9) demonstrates that I_0 is a function of coordinate $\mathbf{x}$:

$$I_0 = I_0(\mathbf{x},\Omega) \tag{10}$$

According to the form of Eq.(8), it can be assumed that T_1 has the following form:

$$T_1(\mathbf{x},\mathbf{y}) = \boldsymbol{N}(\mathbf{y}) \cdot \nabla_{\mathbf{x}} T_0(\mathbf{x}) \tag{11}$$

where $\boldsymbol{N}(\mathbf{y})$ is a dimensionless parameter related to the microscopic structure and thermal conductivity in the periodic RVE. T_1 is the temperature fluctuation. Substitute Eq.(7) and Eq.(11) into Eq.(8), and the $\boldsymbol{N}(\mathbf{y})$ equation can be obtained as:

$$\nabla_{\mathbf{y}} \cdot \left(\mathbf{\Lambda}\nabla_{\mathbf{y}} \boldsymbol{N}\right) + \nabla_{\mathbf{y}} \cdot \mathbf{\Lambda} = 0 \tag{12}$$

In the order of ε^2, there are conduction and radiation equations:

$$\nabla_{\mathbf{x}} \cdot \left(\mathbf{\Lambda}\nabla_{\mathbf{x}} T_0\right) + \nabla_{\mathbf{x}} \cdot \left(\mathbf{\Lambda}\nabla_{\mathbf{y}} T_1\right) + \nabla_{\mathbf{y}} \cdot \left(\mathbf{\Lambda}\nabla_{\mathbf{x}} T_1\right) - 4\kappa\sigma_{\mathrm{B}} T_0^{\,4} + \kappa\int_{4\pi} I_0 \mathrm{d}\Omega = 0 \tag{13}$$

$$\boldsymbol{n} \cdot \left(\nabla_{\mathbf{x}} I_0 + \nabla_{\mathbf{y}} I_1\right) = -\beta I_0 + \frac{\kappa\sigma_{\mathrm{B}}}{\pi} T_0^{\,4} + \frac{\sigma_{\mathrm{s}}\Phi}{4\pi}\int_{4\pi} I_0(\mathbf{x},\Omega')\mathrm{d}\Omega' \tag{14}$$

Next, the macroscopic homogenized conduction and radiation equations can be obtained by taking volumetric average of Eq.(13) and Eq.(14):

$$\nabla_{\mathbf{x}} \cdot (\mathbf{\Lambda}_{\mathrm{eff}} \nabla_{\mathbf{x}} T_0) - \kappa_{\mathrm{eff}} \left(4\sigma_{\mathrm{B}} T_0^{\,4} - \int_{4\pi} I_0 \mathrm{d}\Omega\right) = 0 \tag{15}$$

$$\boldsymbol{n} \cdot \nabla_{\mathbf{x}} I_0 = -\beta_{\mathrm{eff}} I_0 + \frac{\kappa_{\mathrm{eff}}\sigma_{\mathrm{B}}}{\pi} T_0^{\,4} + \frac{(\sigma_{\mathrm{s}}\Phi)_{\mathrm{eff}}}{4\pi}\int_{4\pi} I_0(\mathbf{x},\Omega')\mathrm{d}\Omega' \tag{16}$$

where subscript eff represents homogenized physical parameters, which transfer the microscopic information of the RVE to the macroscopic equations. The homogenized physical parameters including are calculated by Eqs.(17)-(20):

$$\mathbf{\Lambda}_{\mathrm{eff}} = \frac{\int_V \left(\mathbf{\Lambda} + \mathbf{\Lambda}\nabla_{\mathbf{y}} \boldsymbol{N}\right)\mathrm{d}\mathbf{y}}{|V|} \tag{17}$$

$$\beta_{\mathrm{eff}} = \frac{\int_V \beta \mathrm{d}\mathbf{y}}{|V|} \tag{18}$$

$$\kappa_{\text{eff}} = \frac{\int_V \kappa \mathrm{d}\mathbf{y}}{|V|} \tag{19}$$

$$(\sigma_{\text{s}}\Phi)_{\text{eff}} = \frac{\int_V (\sigma_{\text{s}}\Phi)\mathrm{d}\mathbf{y}}{|V|} \tag{20}$$

where V represents the RVE; $|V|$ is the volume of the RVE.

Then, the equation for I_1 can be obtained as:

$$\boldsymbol{n}\cdot\nabla_{\text{y}} I_1 = -(\beta-\beta_{\text{eff}})I_0 + \frac{(\kappa-\kappa_{\text{eff}})\sigma_{\text{B}}}{\pi}T_0^{\,4} + \frac{\left[\sigma_{\text{s}}\Phi-(\sigma_{\text{s}}\Phi)_{\text{eff}}\right]}{4\pi}\int_{4\pi} I_0(\mathbf{x},\Omega')\mathrm{d}\Omega' \tag{21}$$

Finally, by substituting the calculation results of T_0, T_1, I_0 and I_1 into Eq.(3) and Eq.(4), the temperature field and radiative intensity field can be reconstructed.

The heat flux along the direction $\boldsymbol{n}$ is the sum of the heat flux of conduction and radiation:

$$q_{\boldsymbol{n}} = -\boldsymbol{n}\cdot\boldsymbol{\Lambda}\nabla T + \int_{4\pi} I(\mathbf{x},\Omega)(\boldsymbol{n}\cdot\boldsymbol{s})\mathrm{d}\Omega \tag{22}$$

where $q_{\boldsymbol{n}}$ is the total heat flux; $\boldsymbol{s}$ represents the unit vector describing the radiation direction; dΩ is control angle element.

The finite volume method (FVM) is used to simulate coupled conduction-radiation heat transfer process. The effective thermal conductivity $\lambda_{\boldsymbol{n}}$ of the composites along the direction $\boldsymbol{n}$ can be calculated by Eq.(23):

$$\lambda_{\boldsymbol{n}} = -\frac{l}{\Delta T}\cdot\left[\sum_i (q_{\boldsymbol{n},i}\cdot v_i)\Big/\sum_i v_i\right] \tag{23}$$

where l is the thickness of RVE parallel to the direction of heat flow; ΔT is the temperature difference; $q_{\boldsymbol{n},i}$ and v_i represents the heat flux and volume of the i_{th} element respectively.

The convergence criterion for T_0, I_0, I_1, and $\boldsymbol{N}$ is that the relative error between two successive iterations is less than 10^{-6}.

2.2.2 Boundary conditions and material properties.

The periodic boundary condition of the RVEs can ensure continuous temperature and uniform heat flux distribution at the opposite parallel, which can also effectively simulate the periodic structure of the actual composites [7,10]. Two walls along the heat flow direction are set as the heat source and the heat sink. All of the boundary surfaces are all black walls with emissivity of 1.

The radiation absorption and scattering coefficients of SiC, air and carbon fiber are set as constant properties, and the thermal conductivities of carbon fiber and SiC are obtained from the literatures[23,37-38]. In this study, the scattering in the SiC matrix and the air is not considered. The absorption of radiation by the air is ignored.

2.3 Experimental measurement of the effective thermal conductivity

The sample of C/SiC composites is a cylinder with a radius of 12.14 mm and a thickness of 1.92 mm, whose mass is 0.436g. The thermal diffusivity ranging from 100℃ to 900℃ was measured using the laser thermal conductance instrument (NETZSCH LFA 457). The specific heat capacity from 20℃ to 1000℃ was measured by the simultaneous thermal analyzer (NETZSCH STA 449). The effective thermal conductivity k of the sample can be calculated by Eq.(24):

$$k = \alpha\cdot c_{\text{p}}\cdot\rho \tag{24}$$

where α represents the thermal diffusivity; c_{p} is the specific heat capacity, ρ represents the density of the sample.

3. Results and discussion

3.1 Effective thermal conductivities of microscale SiC matrix

A summary of some common theoretical prediction models for calculating the effective thermal conductivity of porous media from literature are listed in Table 2, where λ is the effective thermal conductivity of the porous matrix, λ_m is the thermal conductivity of the matrix, φ is the porosity.

Maxwell-Eucken model assumes that spherical pores with the same diameter are randomly distributed in the matrix, which is used to predict the effective thermal conductivities of two-component materials, especially for the porous matrix [11,39]. The effective medium theory (EMT) is proposed by Bruggeman, which can be used for the matrix with completely random distribution of pores, and the pores are not uniform

in size[12,40]. Besides, the power-law relation and the exponential relation have been widely used for the matrix with the relatively high porosity[41,42].

Table 2 Four models for effective thermal conductivity of porous matrix

Models	Equations	
Maxwell-Eucken	$\lambda=\left(\frac{1-\varphi}{1+\varphi/2}\right)\lambda_m$	(25)
EMT	$\lambda=\left(1-\frac{3}{2}\varphi\right)\lambda_m$	(26)
Power law	$\lambda=(1-\varphi)^{\frac{3}{2}}\lambda_m$	(27)
Exponential	$\lambda=\exp\left(-\frac{3\varphi}{2-2\varphi}\right)\lambda_m$	(28)

To select an applicable formula, numerical simulations are conducted to get effective thermal conductivities with different porosities. Then, a more appropriate model is formulated by comparing simulation results and existing model results. According to the SEM images, the size of the large pores formed by the foaming technique is about 30-50μm, while the size of the small pores in the matrix is only about 2-5μm[9]. Diameter ratio of large to small pores is defined as diametric ratio *d**. Fig.3 shows the RVEs of the matrix, and their diametric ratios are 6 and 10, respectively. The RVE of the matrix contains one large pore and some small pores. The large pore is distributed in the center of the matrix, and then 45 small pores are arranged randomly and uniformly in the rest space of the matrix. All of the neighboring pores can be connected.

The effective thermal conductivity of the matrix is predicted with the diametric ratio ranging from 4 to 10 by the FVM. In order to reduce the influence of matrix anisotropy on the simulation results, the average value of the effective thermal conductivities in the length, width and height directions of the RVE is taken as the calculation results for a specific diametric ratio. The simulation results are show in Fig.4. It can be seen that the diametric ratio has almost no effect on the results, so we assume that the effective thermal conductivity of the matrix depends only on the porosity. The average value with different diametric ratios is taken as the final results.

(a) *d**=6 (b) *d**=10

Fig.3 Samples of the matrix models with random pores of different diametric ratios(*d**)

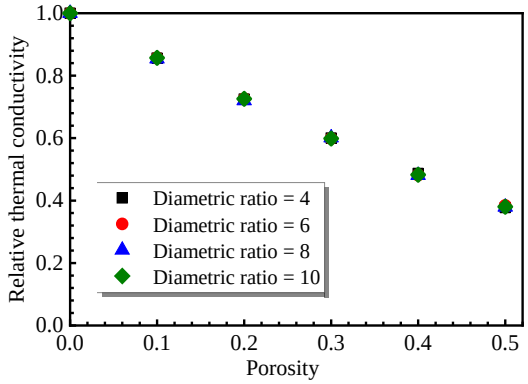

Fig.4 Comparison of the effective thermal conductivity of matrix with different diametric ratios

Fig.5 illustrates that when the porosity is less than 10%, the simulation results are basically consistent with those calculated by the theoretical models. When the porosity is relatively larger, the simulation results

are far from the EMT model and the exponential model, but they are close to the Maxwell–Eucken model and the power-law model.

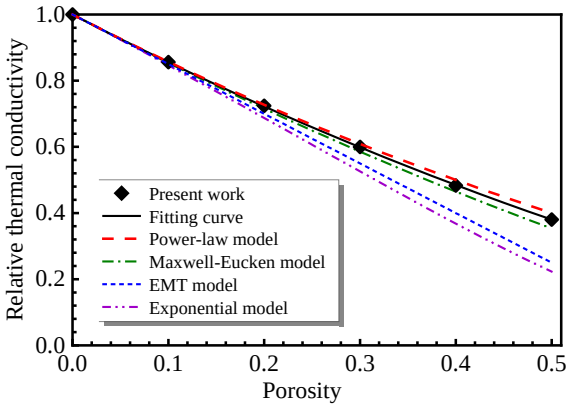

Fig.5 Comparison of the effective thermal conductivity of porous matrix calculated by FVM and theoretical models.

An accurate functional formula of the effective thermal conductivity of the matrix can be obtained by interpolation method, because the FVM curve is just between two existing models, namely Power-law model and Maxwell-Eucken model. Suppose that the modified effective thermal conductivity λ^* of the matrix satisfies:

$$\lambda^*=\left[k\left(\frac{1-\varphi}{1+\varphi/2}\right)+(1-k)(1-\varphi)^{\frac{3}{2}}\right]\lambda_m \tag{29}$$

It can be concluded that the fitting curve is closest to the FVM curve when k=0.57 through the least square method. Eq.(29) is applicable not only to the matrix with randomly distributed pores, but also to the matrix whose pore diametric ratios is less than 10. In the following simulation process, the effective thermal conductivity of the matrix can be directly calculated by Eq.(29).

3.2 Effective thermal conductivities of microscale yarns

The yarn consists of carbon fibers and the SiC matrix. A lot of carbon fibers are uniformly arranged in the SiC matrix. Based on geometric parameters obtained from the SEM images of the C/SiC composites, the RVE model is established as shown in Fig.6. There is a fiber in the center of the RVE, and 1/4 of the fiber in each corner of the RVE model. The thermal conductivity of yarns is anisotropic, and the transverse and longitudinal effective thermal conductivity are simulated respectively.

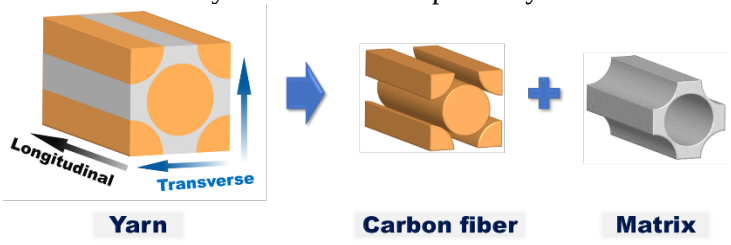

Fig.6 Structural composition of the yarn.

For two-phase composites, the upper limit λ_p and the lower limit λ_s of the effective thermal conductivity are defined by the Parallel and Series models:

$$\lambda_p=\alpha_f\lambda_f+(1-\alpha_f)\lambda_m \tag{30}$$

$$\lambda_s=\frac{\lambda_f\lambda_m}{\alpha_f\lambda_m+(1-\alpha_f)\lambda_f} \tag{31}$$

where α_f is the fiber volume fraction, and λ_f and λ_m are the thermal conductivity of the fiber and the matrix, respectively.

These two models assume that fibers and the matrix are arranged in parallel or in series along the direction of heat flow, which are suitable for layered composites. It is obvious that the longitudinal thermal conductivity of the yarn can be calculated directly by the Parallel model, because the matrix and fibers are arranged "in parallel" along the direction of heat flow. However, the Parallel model and Series model are not directly applicable to the prediction of the transverse thermal conductivity of yarns. We can obtain an

empirical formula of the transverse thermal conductivity by interpolation method. The FVM is used to predict the transverse thermal conductivity λ_t of the RVE of the yarn with different fiber volume fractions. Then, a functional formula is fitted to obtain the relationship between the transverse thermal conductivity and the fiber volume fraction.

$$\lambda_t = f(\alpha_f)\lambda_s + \left[1 - f(\alpha_f)\right]\lambda_p \tag{32}$$

where $f(\alpha_f)$ is a function of the fiber volume fraction α_f, which satisfies $0 < f(\alpha_f) < 1$. λ_p and λ_s are calculated by the Parallel model and Series models respectively. Firstly, the values of $f(\alpha_f)$ is obtained by least square method, and then the function of $f(\alpha_f)$ is fitted by three-order polynomial fit.

In the process of heat-treated, the thermal expansion of the carbon fibers may lead to the compression deformation of the adjacent fiber filaments[9]. According to whether the adjacent carbon fibers are connected, the arrangements of carbon fibers include tight arrangement and loose arrangement， as shown in Fig.7. The fitting formulas of the transverse thermal conductivity for these two arrangements are different, because the heat flux in the yarn drops sharply when the fibers are tightly arranged. The coefficients of the three-order polynomial equation are shown in Table 3.

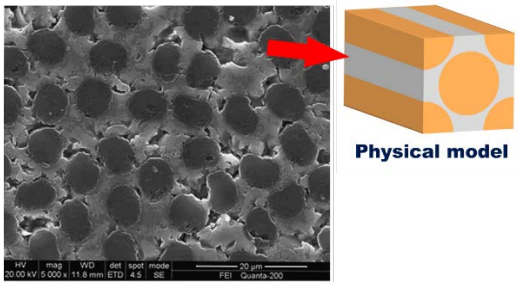

(a) SEM image of loosely arranged fibers[43]

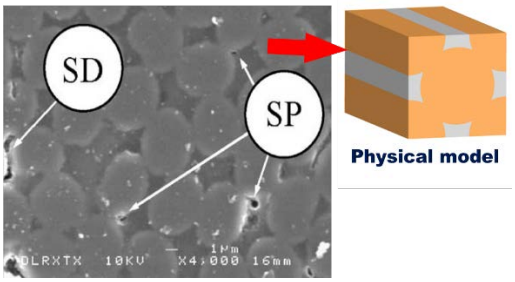

(b) SEM image of a yarn with spherical pores (SP) and shrinkage debonding (SD)[44]

Fig.7 Two kinds of carbon fibers arrangements

Table 3 Coefficients of the regression equations for loose and tight arrangements of carbon fibers

Term of polynomial	Third-order	Second-order	First-order	Constant
Loose arrangement	-5.175	7.126	-3.794	1.400
Tight arrangement	-0.002	0.027	-0.106	0.218

Fig.8 shows the transverse thermal conductivity calculated by the FVM method and the fitting formulas. It can be seen that they are basically the same, so the fitting formulas can be used to calculate the transverse thermal conductivity of yarns with different carbon fiber contents. When the carbon fibers are tightly packed, the transverse thermal conductivity λ_t increases with the increase of temperature, because λ_t is mainly affected by the thermal conductivity of the carbon fiber when α_f is large.

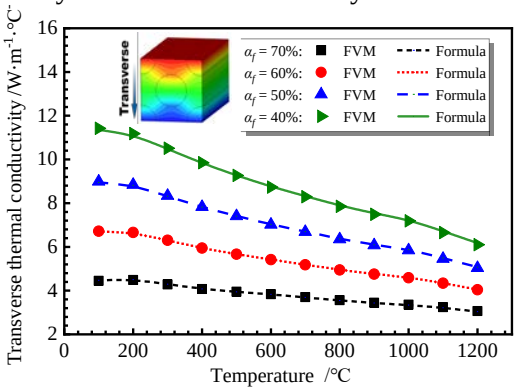

(a) Loose arrangement

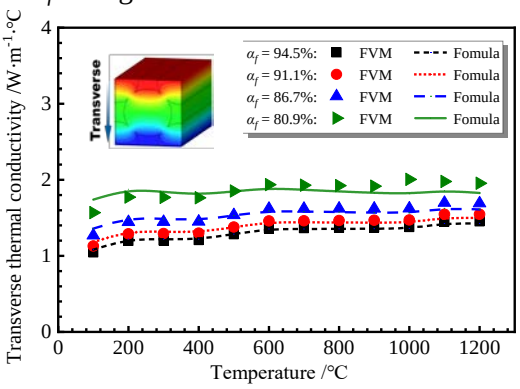

(b) Tight arrangement

Fig.8 Comparison between theoretical formulas Eq.(32) and FVM results in transverse effective thermal conductivity of the RVE of the yarn.

3.3 Effective thermal conductivities of C/SiC composites

Based on the empirical formulas of thermal conductivities of the matrix and the yarn at microscale, the effective thermal conductivity of C/SiC is numerically predicted by using the multiscale coupled conduction-

radiation heat transfer mathematical model. The traditional model directly solves the coupled conduction-radiation heat transfer governing equations, namely Eq.(3) and Eq.(4), in the whole computational domain at mesoscale. The traditional model requires very fine mesh. In order to test the applicability of the proposed multiscale method, the simulation results of the multiscale model are compared with the experimental data and the results of the traditional model. Besides, the computational efficiency of the multiscale model is compared with that of the traditional model.

Taking C/SiC composites at 100℃ as an example (110 °C in high temperature surface and 90 °C in low temperature surface) to present the solution process of the multiscale model. The multiscale model simulates the heat transfer process of the composites at macroscale and mesoscale. The macroscopic physical model of C/SiC composites is formed from 3*3*1 mesoscopic RVEs. Fig.9 shows the macroscopic physical model and the mesoscopic RVE model of plain woven C/SiC composites, with the 247546 mesh elements and the 198480 mesh elements respectively. Meanwhile, the whole composites have 2003010 mesh elements for the computation of the traditional model.

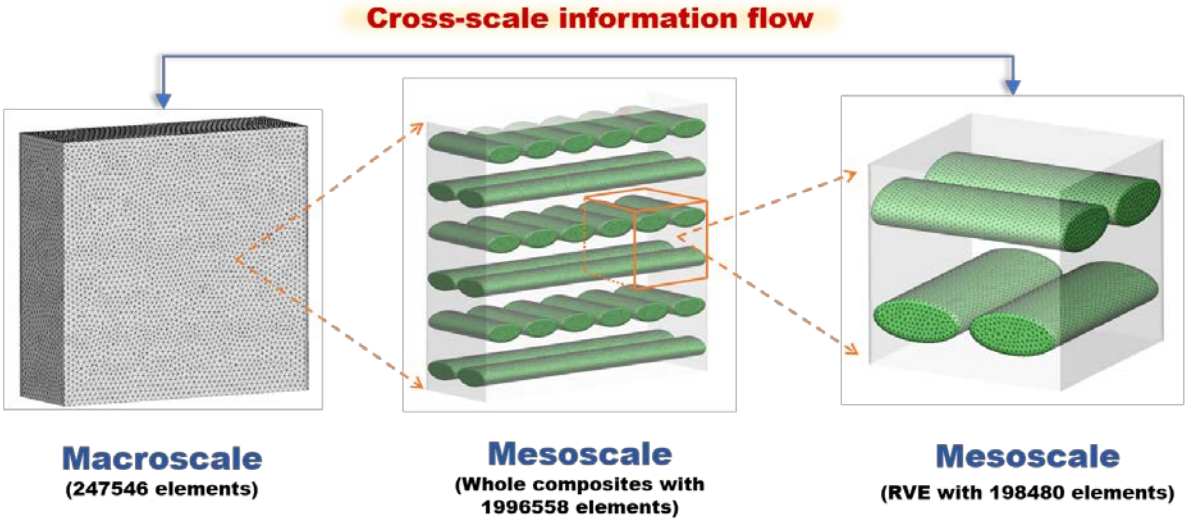

Fig.9 Meshes of the physical models for multiscale numerical simulation

After meshing these physical models at macroscale and mesoscale, Eq.(12) is solved inside the RVE to obtain the calculation result of $N(\mathbf{y})$, as shown in Fig.10. $N(\mathbf{y})$ contains the mesoscale information of the composites, including the structural characteristics and the distribution of thermal conductivities at mesoscale. Then the homogenized parameters can be obtained from Eqs.(17)-(20), as shown in Table 4.

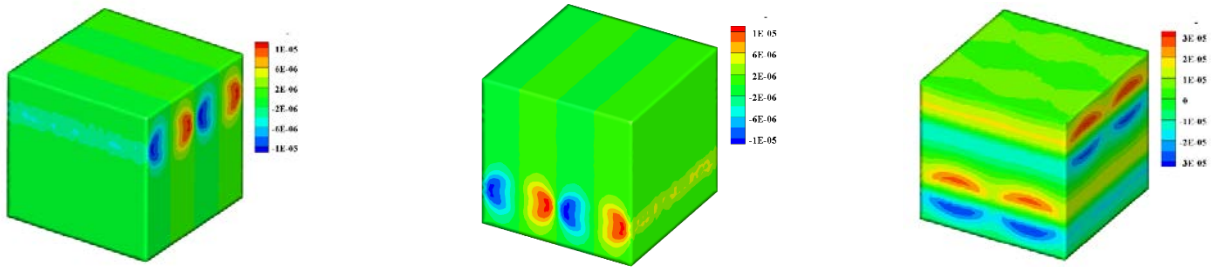

(a) $N(x)$ (b) $N(y)$ (c) $N(z)$

Fig.10 Computational results of $N(\mathbf{y})$

Table 4 Computational results of homogenized parameters in the RVE

$\mathbf{\Lambda}_{\text{eff}}$ / $\text{W}\cdot\text{m}^{-1}\cdot\text{K}^{-1}$	β_{eff} / cm^{-1}	κ_{eff} /cm^{-1}	$(\sigma_s\Phi)_{\text{eff}}$ /cm^{-1}
$\begin{bmatrix} 9.73 & 0 & 0 \\ 0 & 9.73 & 0 \\ 0 & 0 & 5.75 \end{bmatrix}$	254.27	254.20	0.07

Then, we can solve Eq.(15) and Eq.(16) in the macroscopic physical model and obtain the homogenized temperature field T_0 and radiation intensity field I_0. The mesoscale temperature fluctuation T_1 is calculated by Eq.(11). Then based on the homogeneity parameters, T_0, I_0, the radiation fluctuation I_1 is calculated by Eq.(21).

We have solved the homogenized field T_0 and I_0 and the fluctuations T_1 and I_1. The temperature field and radiation intensity field can be reconstructed according to Eq.(3) and Eq.(4), as shown in Fig.11. The heat flux and the effective thermal conductivity are calculated according to Eq.(22) and Eq.(23), respectively.

The effective thermal conductivity prediction results of C/SiC composites by the multiscale model and the traditional model and the experimental data are shown in Fig.12. Comparing with the experimental data, the average relative errors of the multiscale model and the traditional model are 4.13% and 3.87%, respectively. The predicted effective thermal conductivities using the multiscale numerical model are in excellent agreement with those of the experimental data. Therefore, the present multiscale numerical model is validated. As for the CPU time, the traditional simulation takes 8.2h to reach the 10^{-6} convergence criterion. The multiscale simulation consumes totally 1.6h (93.6min), which includes 13.5min for $N(\mathbf{y})$, 40.5min for I_0 and T_0, 1.2min for T_1 and 38.4min for I_1. Therefore, it can be seen that the proposed multiscale numerical method can significantly improve the efficiency the numerical simulation while maintaining its accuracy.

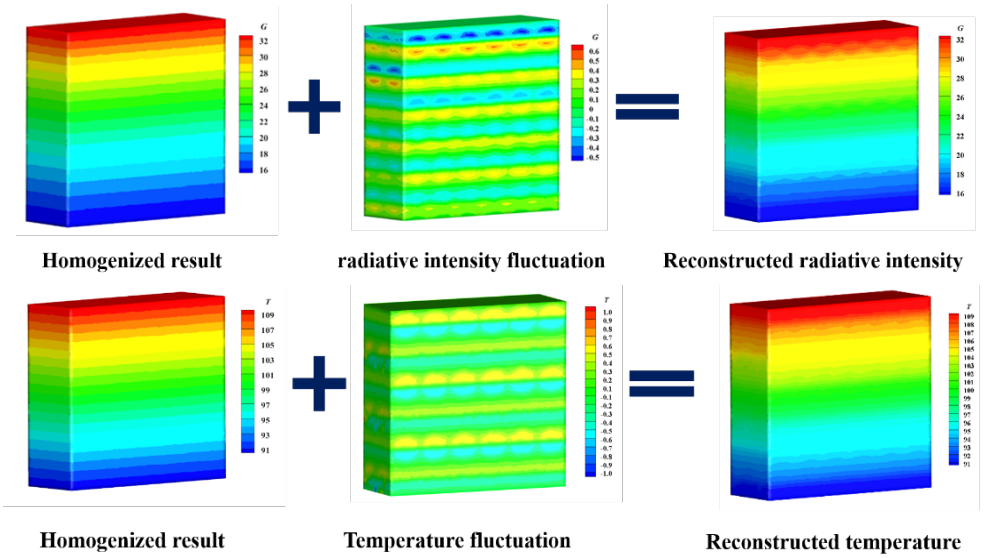

Fig.11 Computational results of the homogenized field T_0 and I_0, the fluctuations T_1 and I_1, and the reconstructed field T and I.

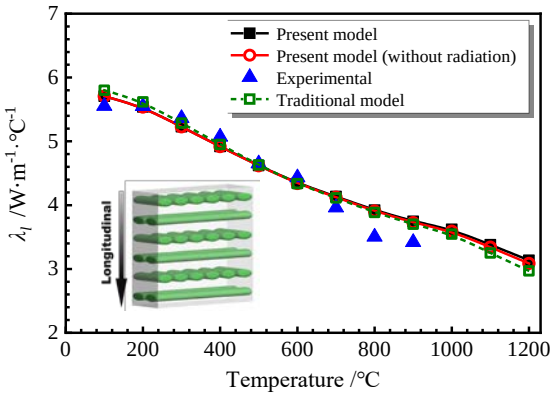

Fig.12 Comparison between multiscale model, traditional model results and experimental data in longitudinal effective thermal conductivity of C/SiC composites.

Fig.13 shows the transverse and longitudinal effective thermal conductivity curves of C/SiC composites with different porosity, and the four curves correspond to the fiber volume fraction of 19.6%, 29.4%, 39.3% and 50.5%, respectively. It can be seen that the effective thermal conductivity (both transverse and longitudinal) has a nearly linear relationship with the porosity, decreasing as the porosity increases. When the porosity increases from 0 to 50%, the longitudinal thermal conductivity decreases by 51.2% and the transverse thermal conductivity decreases by 58.8%. The anisotropy of C/SiC composites is also reflected, which is due to the anisotropy of carbon fibers. The longitudinal thermal conductivity is about 1.4 to 2.1

times that of the transverse thermal conductivity, and the ratio decreases with increasing porosity, so the anisotropy of the composites can be reduced by increasing porosity.

The transverse and longitudinal effective thermal conductivity of C/SiC composites varies with temperature and fiber volume fraction as shown in Fig.14. With the increase of temperature, the longitudinal thermal conductivity decreases about 45.3%, and the transverse thermal conductivity decreases about 50.9%. The Temperature influences the effective thermal conductivity of the composites by affecting the thermal conductivity of carbon fiber and SiC matrix. For different composites, the variation law of the effective thermal conductivity may be different.

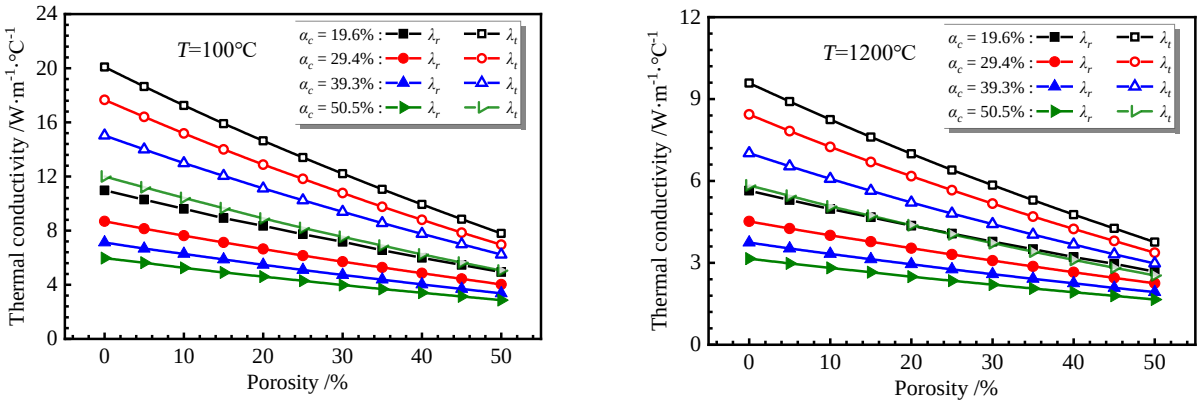

(a) T=100℃ (b) T=1200℃

Fig.13 Longitudinal effective thermal conductivity of C/SiC composites at different matrix porosities and fiber volume fractions.

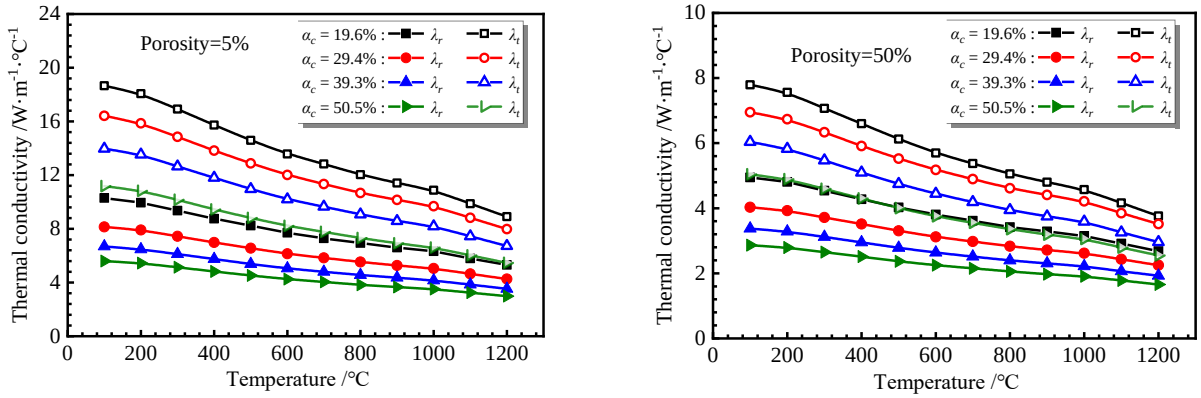

(a) φ=5% (b) φ=50%

Fig.14 Longitudinal effective thermal conductivity of C/SiC composites at different temperatures and fiber volume fractions.

4. Conclusions

In this paper, a multiscale method is proposed to predict the heat transfer properties of composites, which combines the three-scale physical model and multiscale mathematical model. Firstly, the thermal conductivities of yarn and matrix are analyzed at microscale. The empirical formulas are obtained by improving the existing theoretical models. Then, to calculate the effective thermal conductivity of SiC composites, the cross-scale heat transfer mechanism at microscale (RVE scale) and macroscale (the whole composites) is analyzed. By comparing with the traditional model and experimental data, the effectiveness and reasonableness of the proposed multiscale analysis method is proved. This method and conclusions can be extended to other braided composites, which can rapidly and accurately simulate the internal temperature and radiation field, and obtain the heat transfer properties of the material. The main results and contributions of this paper are as follows:

(1) Based on the complex microstructure of composites, an effective thermal conductivity prediction model is established by using a multiscale numerical method, which provided scientific guidance for the heat transfer properties prediction of composites.

(2) The temperature field and radiation intensity field at mesoscale inside the composites can be reconstructed accurately with the error of 4.13%. Comparing with the traditional model, the computational time of the multiscale model can be reduced from more than 8 hours to 1.6 hours.

(3) Porosity, fiber volume fraction and temperature have obvious influence on the effective thermal conductivity of C/SiC composite. Increasing porosity is one of the effective ways to reduce anisotropy of composites.

5. Acknowledgements

This study is supported by the National Numerical Wind Tunnel Project of China (NNW2018ZT2-A04, NNW2020ZT3-A22) and National Natural Science Foundation of China (No. 51906186).

References

[1] Arai Y, Inoue R, Goto K, et al. Carbon fiber reinforced ultra-high temperature ceramic matrix composites: A review[J]. Ceramics International, 2019, 45(12): 14481-14489.
[2] Borkowski L, Chattopadhyay A. Multiscale model of woven ceramic matrix composites considering manufacturing induced damage[J]. Composite Structures, 2015, 126: 62-71.
[3] Chen X, Taylor L W, Tsai L J. An overview on fabrication of three-dimensional woven textile preforms for composites[J]. Textile Research Journal, 2011, 81(9): 932-944.
[4] Naslain R. Design, preparation and properties of non-oxide CMCs for application in engines and nuclear reactors: an overview[J]. Composites Science and Technology, 2004, 64(2): 155-170.
[5] Kumar S, Kumar A, Sampath K, et al. Fabrication and erosion studies of C–SiC composite Jet Vanes in solid rocket motor exhaust[J]. Journal of the European Ceramic Society, 2011, 31(13): 2425-2431.
[6] Xu H, Zhang L, Cheng L. Effects of yarn size and Z-yarn density on the interlaminar shear properties of two Z-reinforced 3D C/SiC composites[J]. Materials & Design, 2014, 64: 434-440.
[7] Gou J J, Dai Y J, Li S, et al. Numerical study of effective thermal conductivities of plain woven composites by unit cells of different sizes[J]. International Journal of Heat and Mass Transfer, 2015, 91: 829-840.
[8] Sheikh M A, Taylor S C, Hayhurst D R, et al. Microstructural finite-element modelling of a ceramic matrix composite to predict experimental measurements of its macro thermal properties[J]. Modelling and Simulation in Materials Science and Engineering, 2001, 9(1): 7.
[9] Berbon M Z, Dietrich D R, Marshall D B, et al. Transverse thermal conductivity of thin C/SiC composites fabricated by slurry infiltration and pyrolysis[J]. Journal of the American Ceramic Society, 2001, 84(10): 2229-2234.
[10] Li H, Li S, Wang Y. Prediction of effective thermal conductivities of woven fabric composites using unit cells at multiple length scales[J]. Journal of Materials Research, 2011, 26(3): 384.
[11] Hashin Z, Shtrikman S. A variational approach to the theory of the effective magnetic permeability of multiphase materials[J]. Journal of applied Physics, 1962, 33(10): 3125-3131.
[12] Landauer R. The electrical resistance of binary metallic mixtures[J]. Journal of Applied Physics, 1952, 23(7): 779-784.
[13] Gibson I J, Ashby M F. The mechanics of three-dimensional cellular materials[J]. Proceedings of the royal society of London. A. Mathematical and physical sciences, 1982, 382(1782): 43-59.
[14] Pabst W, Gregorová E. Mooney-type relation for the porosity dependence of the effective tensile modulus of ceramics[J]. Journal of materials science, 2004, 39(9): 3213-3215.
[15] Zhou L C, Sun X H, Chen M W, et al. Multiscale modeling and theoretical prediction for the thermal conductivity of porous plain-woven carbonized silica/phenolic composites[J]. Composite Structures, 2019, 215: 278-288.
[16] Pilling M W, Yates B, Black M A, et al. The thermal conductivity of carbon fibre-reinforced composites[J]. Journal of Materials Science, 1979, 14(6): 1326-1338.
[17] Clayton W. Constituent and composite thermal conductivities of phenolic-carbon and phenolic-graphite ablators[C]//12th Structures, Structural Dynamics and Materials Conference. 1971: 380.
[18] Maxwell J C. Electricity and magnetism[M]. New York: Dover, 1954.
[19] Kumlutaş D, Tavman I H, Çoban M T. Thermal conductivity of particle filled polyethylene composite materials[J]. Composites science and technology, 2003, 63(1): 113-117.
[20] Thiele A M, Kumar A, Sant G, et al. Effective thermal conductivity of three-component composites containing spherical capsules[J]. International Journal of Heat and Mass Transfer, 2014, 73: 177-185.

[21] Ioannou I, Hodzic A, Gitman I M. Numerical investigation of thermal and thermo-mechanical effective properties for short fibre reinforced composite[J]. Applied Composite Materials, 2017, 24(5): 999-1009.
[22] Gou J J, Zhang H, Dai Y J, et al. Numerical prediction of effective thermal conductivities of 3D four-directional braided composites[J]. Composite Structures, 2015, 125: 499-508.
[23] Liu Y, Qu Z G, Guo J, et al. Numerical study on effective thermal conductivities of plain woven C/SiC composites with considering pores in interlaced woven yarns[J]. International Journal of Heat and Mass Transfer, 2019, 140: 410-419.
[24] Bensoussan A, Lions J L, Papanicolaou G. Asymptotic analysis for periodic structures[M]. American Mathematical Soc., 2011.
[25] Weinan E. Principles of multiscale modeling[M]. Cambridge University Press, 2011.
[26] Cao L, Luo J. Multiscale Numerical Methods for Heat and Mass Transfer Problems of Composite Porous Media with a Periodic Structures[J]. JOURNAL OF ENGINEERING THERMOPHYSICS, 2000, 21(5): 610-614.
[27] Liu S, Zhang Y. Multi-Scale Analysis Method for Thermal Conductivity of Porous Material with Radiation[J]. Multidiscipline Modeling in Materials and Structures, 2006.
[28] Allaire G, El Ganaoui K. Homogenization of a conductive and radiative heat transfer problem[J]. Multiscale Modeling & Simulation, 2009, 7(3): 1148-1170.
[29] Yang Z, Cui J, Nie Y, et al. The second-order two-scale method for heat transfer performances of periodic porous materials with interior surface radiation[J]. Computer Modeling in Engineering & Sciences(CMES), 2012, 88(5): 419-442.
[30] Huang J, Cao L, Yang C. A multiscale algorithm for radiative heat transfer equation with rapidly oscillating coefficients[J]. Applied Mathematics and Computation, 2015, 266: 149-168.
[31] Haymes R, Gal E. Iterative multiscale approach for heat conduction with radiation problem in porous materials[J]. Journal of Heat Transfer, 2018, 140(8).
[32] Allaire G, Habibi Z. Homogenization of a conductive, convective, and radiative heat transfer problem in a heterogeneous domain[J]. SIAM Journal on Mathematical Analysis, 2013, 45(3): 1136-1178.
[33] Del Puglia P, Sheikh M A, Hayhurst D R. Classification and quantification of initial porosity in a CMC laminate[J]. Composites Part A: Applied Science and Manufacturing, 2004, 35(2): 223-230.
[34] Xu H, Zhang L, Wang Y, et al. The effects of Z-stitching density on thermophysical properties of plain woven carbon fiber reinforced silicon carbide composites[J]. Ceramics International, 2015, 41(1): 283-290.
[35] Xu Y, Ye H, Zhang L, et al. Investigation on the effective thermal conductivity of carbonized high silica/phenolic ablative material[J]. International Journal of Heat and Mass Transfer, 2017, 115: 597-603.
[36] Tong Z X, Li M J, Yu Y S, et al. A Multiscale Method for Coupled Steady-State Heat Conduction and Radiative Transfer Equations in Composite Materials[J]. Journal of Heat Transfer, 2021.
[37] Zahida M, Sharmaa R, Bhagat AR, et al. Micro-structurally informed finite element analysis of carbon/carbon composites for effective thermal conductivity[J]. Composite Structures, 2019, 226: 111221.
[38] Sun Z, Shan Z, Shao T. A comparative study for the thermal conductivities of C/SiC composites with different preform architectures fabricating by flexible oriented woven process[J]. International Journal of Heat and Mass Transfer, 2021, 170: 120973.
[39] Qiu L, Zou H, Tang D, et al. Inhomogeneity in pore size appreciably lowering thermal conductivity for porous thermal insulators[J]. Applied Thermal Engineering, 2018, 130: 1004-1011.
[40] Kirkpatrick S. Percolation and conduction[J]. Reviews of modern physics, 1973, 45(4): 574.
[41] Gibson I J, Ashby M F. The mechanics of three-dimensional cellular materials[J]. Proceedings of the royal society of London. A. Mathematical and physical sciences, 1982, 382(1782): 43-59.
[42] Pabst W, Gregorová E. Mooney-type relation for the porosity dependence of the effective tensile modulus of ceramics[J]. Journal of materials science, 2004, 39(9): 3213-3215.
[43] Xiang Y, Li W, Wang S, et al. Oxidation behavior of oxidation protective coatings for PIP–C/SiC composites at 1500° C[J]. Ceramics International, 2012, 38(1): 9-13.
[44] Del Puglia P, Sheikh M A, Hayhurst D R. Classification and quantification of initial porosity in a CMC laminate[J]. Composites Part A: Applied Science and Manufacturing, 2004, 35(2): 223-230.